

# EFFECTIVE CHANNEL CODING OF SERIALY CONCATENATED ENCODERS AND CPM OVER AWGN AND RICIAN CHANNELS

Manjeet Singh (ms308@eng.cam.ac.uk)  
Ian J. Wassell (ijw24@eng.cam.ac.uk)

Laboratory for Communications Engineering  
Department of Engineering  
University of Cambridge

## ABSTRACT

*A generic  $M$ -ary continuous phase modulation (CPM) scheme, with a modulation index of  $h = 1/M$ , can be modeled by a continuous-phase encoder (CPE) followed by a memoryless modulator (MM), where the CPE is linear over the ring of integers modulo  $M$ . By designing a channel encoder (CE), which is a convolutional encoder, to operate over the same ring of integers modulo  $M$ , the CE and the CPE can be combined to create another convolutional encoder called an extended CE. In this paper, a  $1/2$  rate CE over the ring of integers modulo 4 is combined with a 4-ary CPM scheme whose modulation index is  $h = 1/4$ . Using this trellis coded modulation design, the paper explains the design of an effective serially concatenated channel coded system, where the inner encoder is the extended CE and the outer encoder is another convolutional encoder. Simulations show that good results are obtainable by concatenating an outer quaternary convolutional encoder with the quaternary extended CE.*

## I. INTRODUCTION

Since the pioneering work of Ungerboeck in 1982, trellis-coded modulation (TCM) has become an effective coding technique for bandlimited channels. By using TCM with memoryless modulations, such as  $M$ -ary phase shift keying (MPSK) or quadrature amplitude modulation (QAM), significant coding gains can be achieved without bandwidth expansion. Studies have also been done that combine encoders with memory modulation schemes [1]. One such scheme is continuous phase modulation (CPM).

CPM is a form of constant-envelope digital modulation and therefore of interest for use with nonlinear and/or fading channels. The inherent bandwidth- and energy efficiency makes CPM a very attractive modulation

scheme. Furthermore, CPM signals have good spectral properties due to their phase continuity.

Besides providing spectral economy, CPM schemes exhibit a “coding gain” when compared to PSK modulation. This “coding gain” is due to the memory that is introduced by the phase-shaping filter and the decoder can exploit this. CPM modulation exhibits memory that resembles in many ways how a convolutionally encoded data sequence exhibits memory - in both cases, a “trellis” can be used to display the possible output signals (this is why convolutional encoders are used with CPM in this paper).

Massey in [2] suggested that CPM could be decomposed into two parts: a continuous phase encoder (CPE) with memory, and a memoryless modulator (MM). Such decomposition has two advantages [4]. Firstly, the “encoding” operation can be studied independently of the modulation. The second advantage is that the isolation of the MM would allow the cascade of the MM, the waveform channel (e.g. additive white Gaussian noise (AWGN)) and the demodulator to be modeled as a discrete memoryless channel.

In [3, 4, 5], Rimoldi derived a generic decomposition model of an  $M$ -level CPFSK, comprising a CPE and an MM. He showed that the CPE is a linear (modulo some integer  $M$ ) time-invariant encoder and the MM another time-invariant device. It is then of interest to optimally combine a convolutional coder with the CPE to create a trellis coded modulation scheme.

The mathematics of how to combine a convolutional encoder with the CPE without the use of a mapper is given in [6]. One condition, among others, is that both the encoder and the CPE must operate over the same algebra. This is unlike the usual approach where mappers are pertinent [1, 7].

In this paper, we combine a 4-ary convolutional encoder, hereafter called a *channel encoder* (CE), with a 4-ary CPE. Such a combination is called an extended CE and is effectively a convolutional encoder. We compare the performance of 2 channel coding configurations. In both configurations, a  $\frac{1}{2}$  rate CE (convolutional encoder) over the ring of integers modulo 4 is combined with a 4-ary CPM scheme. More specifically, we consider a 2 raised cosine (2RC) scheme with a modulation index of  $h = \frac{1}{4}$ .

An effective serially concatenated channel coding system is designed, where the inner encoder is the extended CE and the outer encoder is another convolutional encoder. Both soft and hard decoding techniques are investigated. The soft output information from the inner Soft-Output Viterbi Algorithm (SOVA) is used to enhance the performance of the outer soft input Viterbi decoder.

## II. SYSTEM DESIGN

The section explains the design of the two configurations considered in the study, both of which are based on serially concatenated coding techniques. In the first configuration shown in Figure 1:

a. The outer encoder is a binary convolutional encoder while the inner encoder (the extended CE) is a quaternary convolutional encoder. As both the inner and outer encoders do not operate over the same algebra, a binary-to-quaternary mapper is required.

b. The inner decoder is a quaternary SOVA. This provides soft output information, which is used by the binary soft input outer decoder, to enhance its decoding performance. A quaternary to binary mapper is required to convert the symbols from quaternary to binary.

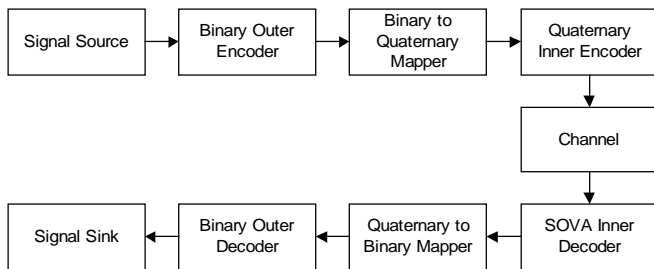


Figure 1. Block diagram of the serially concatenated coding system using a binary outer encoder.

For the second configuration shown in Figure 2:

a. The outer encoder is a quaternary convolutional encoder while the inner encoder is the same quaternary encoder as that employed in Figure 1. No mapper is required here as both the encoders operate over the same algebra structure.

b. Both the inner and outer quaternary decoders perform hard decision decoding.

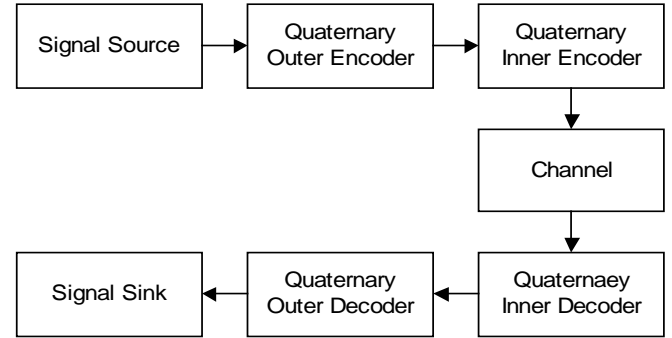


Figure 2. Block diagram of the serially concatenated coding system using a quaternary outer encoder.

### A. Design of the extended CE

Figure 3 shows the design of the extended CE. For the purpose of system evaluation, a 2RC (partial-response) scheme with  $h = \frac{1}{4}$  ( $M = 4$ ) was implemented using the baseband decomposed CPM model. The CPE has two memory (delay) cells. One cell stores the previous transmitted symbol while the other memory cell stores the sum (mod 4) of all previously transmitted symbols. As the phase response of the incoming signal lasts two symbol intervals ( $L = 2$ ), intersymbol interference is introduced.

The extended CE is a  $\frac{1}{2}$  quaternary convolutional encoder. It has 3 memory cells (memory cells D1 and D2 form part of the CPE) and generates 64 states ( $4^3$ ). As there are 4 branches/ waveforms emanating from and arriving at each state and each “analog” waveform is made of 8 samples, a total of  $8 \times 4 \times 64 = 2048$  waveform samples would require processing for the extended CE at each iteration of the Viterbi algorithm.

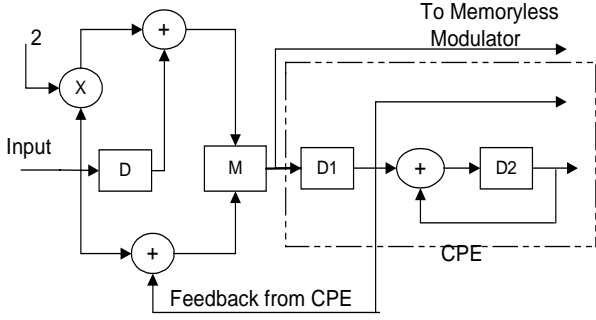


Figure 3.  $\frac{1}{2}$  rate extended CE with feedback from the CPE.  $D$  denotes a memory cell while  $M$  denotes a multiplexer. Additions are all modulo 4.  $D1$  and  $D2$  are the memory cells of the CPE.

By designing the CE to operate over the same algebra as the CPE, no mapper is required to link them. This allows the state of the CPE to be fed back and be used by the CE enabling the use of a CE with a shorter constraint length. Such a combination is called an extended CE, as the CPE is now an extension of the CE.

### B. Design of the Memoryless Modulator

The raised cosine (RC) phase shaping function is implemented using two finite impulse response (FIR) digital filters, FIR filter A and FIR filter B as shown in Figure 4. In this study, each output waveform is made up of eight samples.

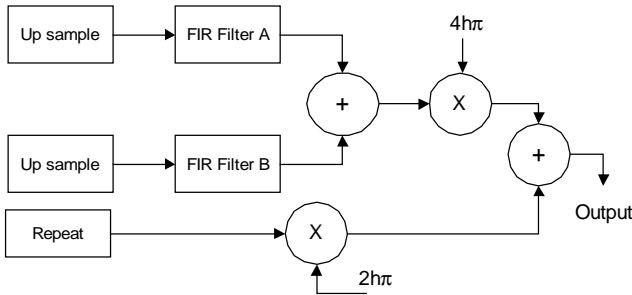


Figure 4. Block diagram of the memoryless modulator. The Up Sample and Repeat blocks increase the samples of the input signals by a factor of 8.  $h$  denotes the modulation index.

### C. Design of the Outer Encoders

In Figure 1, the outer encoder is a  $(2, 1, 5)$  binary convolutional encoder. This is a  $\frac{1}{2}$  rate encoder with a constraint length of 5 and a generator polynomial of  $(50,$

$44)_{10}$ . The quaternary outer convolutional encoder in Figure 2 is similar in design to the extended CE except that there are no outputs to the MM.

### D. Design of the Viterbi Decoders

A general overview of the Viterbi decoder is shown in Figure 5. Its design is based on the concept in [8]. The design of both the hard decoder and the SOVA is basically the same.

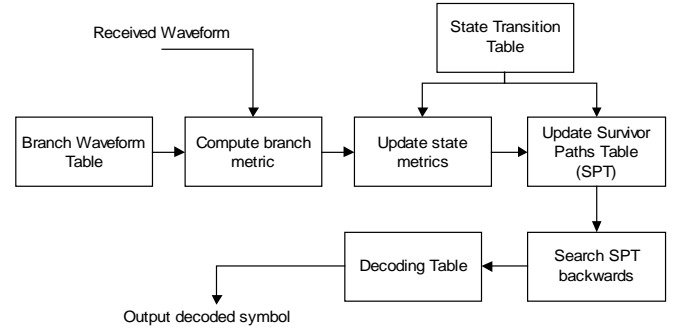


Figure 5. High-level diagram of the Viterbi Decoders

When a waveform is received, (corrupted by additive noise or fading), the Euclidean distances between it and all possible waveforms are calculated. These distances (or branch metrics) serve as a probability that a given waveform/ symbol was actually sent. However, these branch metrics are not used in isolation. They are used in conjunction with the probabilities (state metrics) associated with the states of the trellis that each of the branches departs from. In this way, the Euclidean distance between the entire received sequence and the most likely path through the trellis can be calculated on a symbol-by-symbol basis.

To implement the demodulator, three tables are required. These were generated by the modulator (extended CE and MM) and are used by the demodulator to decode the received symbol sequence. The three tables are:

- State Transition Table - which takes as its inputs the current state and input symbol and outputs the next state.
- Waveform Table – which takes as inputs the current state and symbol input and generates the output waveform.
- Decoding Table – which takes as its inputs the current state and previous state and outputs the transmitted symbol.

It is assumed that there are no parallel transitions between states. The advantage of using these tables is that for the same value of  $L$  the Viterbi decoders need not be redesigned for each new scheme to accommodate more or less states or a different symbol alphabet size.

Apart from outputting the decoded symbol, the SOVA, in the first configuration, also outputs reliability information, which is used to improve the performance of the outer decoder. As there are 4 branches departing and arriving at each state, the reliability information was calculated based on the lowest and highest cumulative metric through the trellis.

### III. SIMULATIONS AND RESULTS

The entire coding system was built in software and tested using Monte Carlo based simulations. The results obtained are in terms of the bit error rate (BER) as a function of the signal to noise ratio (SNR).

The simulations were executed in two types of channels, the additive white Gaussian noise (AWGN) channel and the Rician fading channel. For the simulations in the Rician fading channel, the channel was designed with a Rician parameter ( $K$ ) of 10. This parameter is defined as:

$$K = \frac{\text{power of dominant path}}{\text{power in scattered path}} \quad (1)$$

When  $K = 0$ , the channel is Rayleigh, and if  $K$  is infinite, the channel is Gaussian. The fades have a high probability of being very deep when  $K = 0$  to being very shallow when  $K = 32$  (approaching Gaussian) [9].

In all the simulations, a normalized bandwidth of  $BT_s = 1.2$  was assumed where  $B$  is the bandwidth and  $T_s$  the symbol duration. For the quaternary 2RC scheme, this bandwidth contains approximately 99.97% of the total power.

In both configurations, the overall code rate is  $\frac{1}{4}$  (both the inner and outer encoders have a code rate of  $\frac{1}{2}$ ). However in terms of the number of states, the binary outer encoder, in the first configuration, has 32 states while the outer encoder in the second configuration has 64 states. The inner encoder (the extended CE) in both configurations has 64 states.

Results of all the simulations are shown graphically in Figure 6. For the 2<sup>nd</sup> configuration, a BER of  $1.4 \times 10^{-4}$  at 1.6dB SNR was achievable in the AWGN channel and this was without the use of an interleaver, linking the 2

encoders. With a 10 X10 block interleaver, a BER of  $2.8 \times 10^{-4}$  was obtained at 0.6 dB SNR and with a 50 X 50 block interleaver, the BER reduced to  $9.9 \times 10^{-5}$  at 0.2dB SNR. (Note: BER results using interleavers are not shown in the figure)

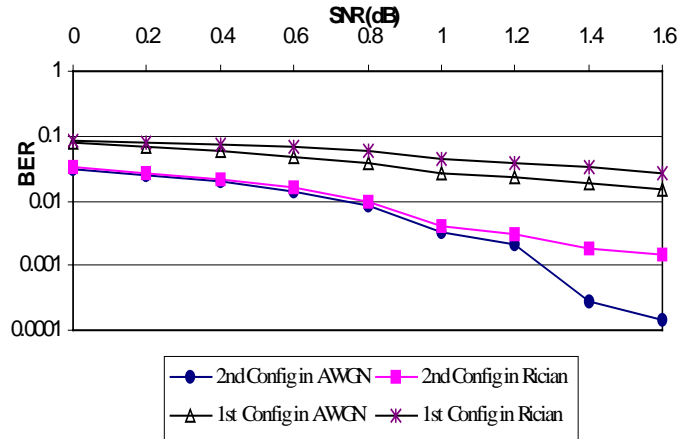


Figure 6. BER as a function of SNR (dB).

The graph clearly shows the superiority of the second configuration (using a quaternary outer encoder) over the first (which used a binary outer encoder) even though the latter used a SOVA inner decoder. A possible reason may be the fact that the outer code utilized a binary encoder instead of a much more natural convolutional encoder over the ring of integers modulo 4. As a result, the quaternary symbols output by the inner decoder had to be mapped back into binary symbols. Whenever a symbol error occurred, two consecutive bit errors are created. Furthermore, these consecutive errors are correlated and are assigned the same reliability information

### IV. DISCUSSION AND CONCLUSION

Previous works [4, 6] have suggested decomposing a CPM modulator and combining the CPE with a CE naturally i.e. without a mapper. To enable this, both the CE and the CPE must operate over the same algebra structure. In our research, we have designed an effective serially concatenated coding system and tested it in AWGN and Rician channels.

The results, in terms of BER, of the second configuration were clearly superior to those of the first. A possible explanation could be the mapping that was necessary between the binary and quaternary symbols in

the latter configuration. With interleavers, the second configuration exhibited very good results. The main potential area of application of the 2<sup>nd</sup> configuration is the improvement of already established standards, for example GSM and cellular digital packet data.

### ACKNOWLEDGEMENTS

The authors would like to thank the Laboratory for Communications Engineering (Cambridge University) for the use of their equipment in the research and the Center for Wireless Communications (National University of Singapore) for their assistance.

### REFERENCES

- [1] J.B. Anderson, T. Aulin and C.E. Sundberg, "Digital Phase Modulation", New York: Plenum, 1986.
- [2] J.L. Massey, "*The how and why of channel coding*," in Proc. Int. Zurich Seminar, Mar.1984, pp. F11(67)-F17(73).
- [3] B. Rimoldi, "*A decomposed approach to CPM*," IEEE Trans. Inform. Theory, vol.34, pp.260-270, Mar.1988.
- [4] B. Rimoldi, "*Continuous phase modulation and coding from bandwidth and energy efficiency*," PhD dissertation, Swiss Fed. Inst. Technol., 1988.
- [5] B. Rimoldi, "*Design of coded CPFSK modulation system for bandwidth and energy efficiency*," IEEE Trans. Commun., vol.37, pp. 897-905, Sept.1989.
- [6] Quinn Li, "*On bandwidth and energy efficient digital modulation schemes*," PhD dissertation, Sever Institute, University of Washington, 1996.
- [7] S.V. Pizzi and S.G. Wilson, "*Convolutional coding combined with Continuous Phase Modulation*," IEEE Trans. Commun., vol.33, pp.20-29, Jan.1985.
- [8] Candido J.A. Levita, "*Investigation of Coded and Uncoded CPM based Wireless Communication Systems*," PhD dissertation, School of Engineering, University of Huddersfield, 1999.
- [9] R. Steele (Editor), *Mobile Radio Communications*, London: Pentech Press, 1994.